Monte Carlo simulation of a multiparticle imaging Cherenkov counter

Ringnér, Markus

1993

Document Version:
Publisher's PDF, also known as Version of record

Monte Carlo simulation of a multiparticle imaging Cherenkov counter

CERN summer student project
in the NA44 experiment

Markus Ringner

26 August 1993

Abstract

A simulation study of a new Cherenkov detector for the NA44 experiment is presented. Different positions and configuratons of the counter are evaluated. The best particle identification performance is achieved with a CaF_2 window and with the chamber placed in front of hodoscope 3 (H3).

1 Introduction

1.1 Cherenkov radiation and detectors

In the following I will give a short description of Cherenkov radiation. A more detailed description can be found for example in [1].

If a charged particle moves through a medium faster than the phase velocity of light in that medium, it will emit photons along its path. The photons will be emitted in an angle determined by the velocity of the particle and the refractive index of the medium according to the following formula (See Fig. 1):

$$\cos\Theta = 1/(\beta n) \tag{1}$$

where Θ is the half angle of the Cherenkov cone,
β the velocity of the particle expressed in the vacuum velocity of light,
and n the refractive index.

This effect is generally used in detectors in two different ways. Either the presence/absence of photons (in threshold Cherenkov counters), or a direct measurement of the Cherenkov angle (Differential or Ring-Image Cherenkov counters) is used to give information about the particle. The Cherenkov photons are normally deflected by a mirror, which the particle goes through, and then they are detected (see Fig. 1).

The energy spectra of the photons is proportional to $1/\lambda^2$. This means that gaining in the detectors efficiency for short wavelengths gives a significant increase in the number of detected photons.

The detector that has been simulated is a gas imaging Cherenkov counter which will be used to identify pions and kaons. The pressure of the gas is set, so that the corresponding index of refraction, results in a threshold to distinguish pions and kaons with a momentum of 3-10 GeV/c. At the same momentum the lighter pions will travel faster and emit Cherenkov radiation, while the heavier kaons are too slow. In addition the positions of the photons are measured and using this information the particles can be identified.

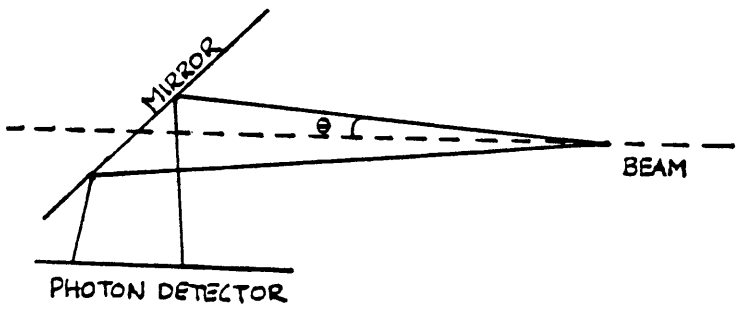

Figure 1: The geometry of Cherenkov radiation and detection. The mirror reflects the photons into a photon detector.

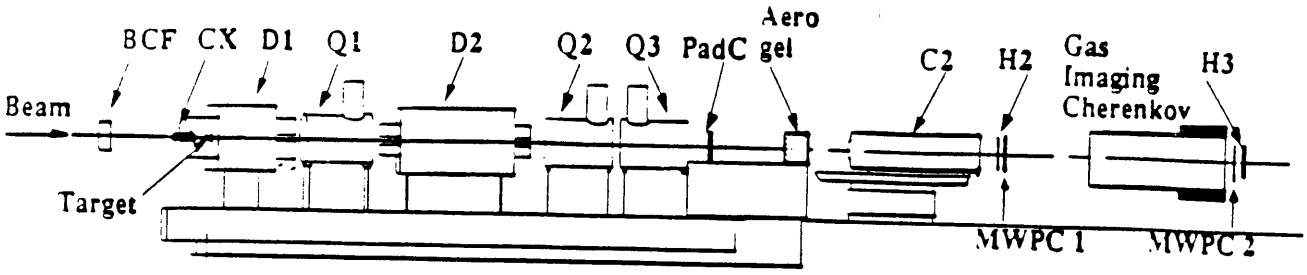

Figure 2: NA44 experimental layout for the Pb beams in 1994.

1.2 The experimental setup

The CERN NA44 experiment is building a multiparticle Cherenkov detector which will be used to identify the heavier particles in high particle multiplicity events, dominated by pions. The NA44 experimental setup is shown in Fig. 2. It is a focussing spectrometer developed for the ultra-relativistic heavy-ion beams at the CERN Super Proton Synchrotron (SPS). It measures one-particle spectra and two-particle correlations. The ions hit a nuclear fixed target and the secondary particles produced at the target are deflected and focussed by a series of dipole and quadrupole magnets. The spectrometer covers only a small part of phase space and therefore only a few particles per event are detected in this high particle-multiplicity environment [2].

In the fall of 1994 a lead-ion beam will be made available at the SPS. In central lead on lead collisions the multiplicity is approximately five times higher than in central sulphur on lead collisions, which is the heaviest projectile-target system studied so far in NA44. The new Cherenkov counter will replace an existing threshold counter, which will have difficulties to cope with the higher multiplicities.

2 Description of the detector

The design can be seen in Fig. 3. Particles travel through the detector from right to left. The photons emitted by the pions are reflected by the mirror and after having passed through a window they are detected by one of the two photodetectors.

The radiator gas used is C_4F_{10} at atmospheric pressure. It has very good UV transmission, down to $\approx$160 nm.

The photon detector is a thin Multi Wire Proportional Chamber (MWPC) with a two-dimensional pad structure readout as can be seen in Fig. 4. Photons enter through the window and are converted into electrons between the two meshes. The gas in the chamber is methane with a TMAE mixture to convert the photons. The released electron then passes the second mesh, ionizing gas molecules on it's way. The sense wires are held at a high voltage and the electric field is at it's maximum on the surface of the sense wires and decreases rapidly outwards. Very close to the wire the field is strong enough for multiplication and an avalanche develops [3]. This results in a signal only on the sense wire closest to the electron trajectory. The released ions give an induced charge on the cathode pads below the wire.

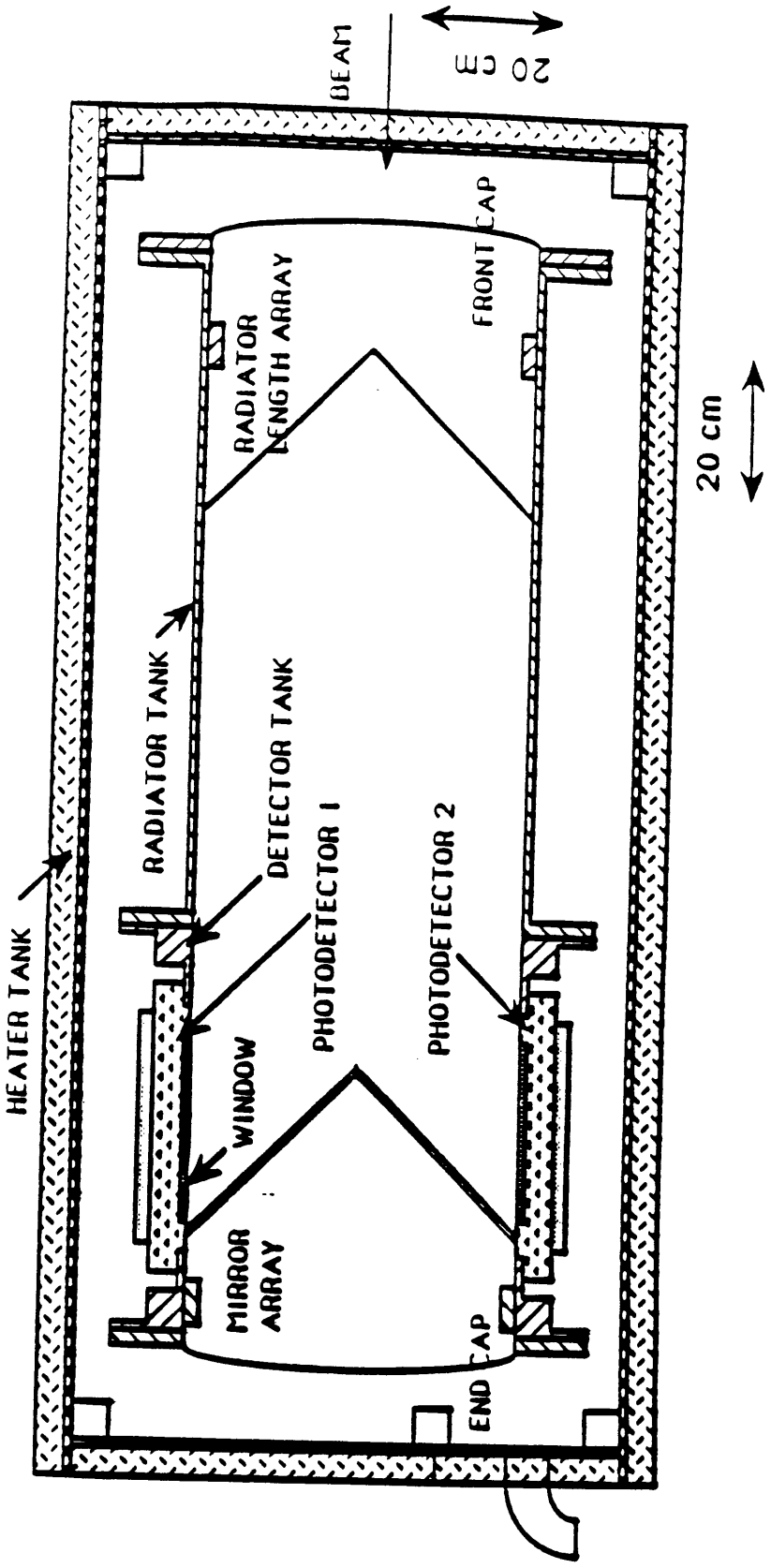

Figure 3: Layout of the gas imaging Cherenkov counter.

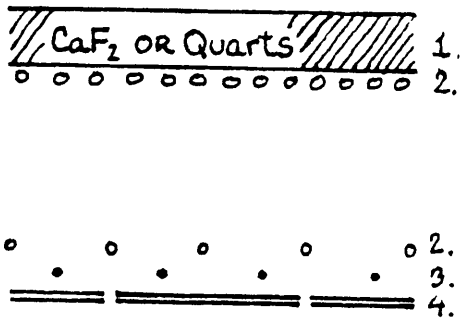

Figure 4: The pad chamber. (1) entrance window, (2) meshes, (3) sense wires, (4) pads

The mean number of detected photoelectrons in the case that the Cherenkov angle (or equivalently the index of refraction) is nearly constant over the useful range of TMAE conversion is given by the following relation:

$$N_{p.e} = LN_0 \sin^2 \Theta \tag{2}$$

with N_0, the factor of merit given by:

$$N_0 = 370 \int \epsilon(E) dE \;\; cm^{-1} eV^{-1} \tag{3}$$

where L is the pathlength of the particle in the radiator,
E the energy of the photon,
and ϵ the total efficiency, taking into account all sources of detection losses of photons and photoelectrons through the detector.

Using a V-shaped mirror (see Fig. 3) reduces the sizes of the windows and the photon detectors compared to a traditional flat mirror (see Fig. 1) with one large photon detector.

3 The simulation

3.1 General description

Events are generated using real tracks of particles with momentum 4 GeV/c from previous data taking. Tracks are randomly chosen to create events with multiplicity 5 and a kaon/pion ratio of 10% is used. The readout cathode is segmented into pads of 8x8mm^2. Noise photons are generated, up to 4 per track, flatly distributed all over the padarray. The particles and photons are tracked through the detector.

The induced relative charges on the pads are calculated according to a two-dimensional gaussian.

$$G(x, y) = e^{-(x^2+y^2)/(2*\sigma^2)} \tag{4}$$

A value of σ=1.5mm was used [4]. A look up table has been made by varying the position of the avalanche along the wire in steps of 1mm and normalizing the sum for each position to

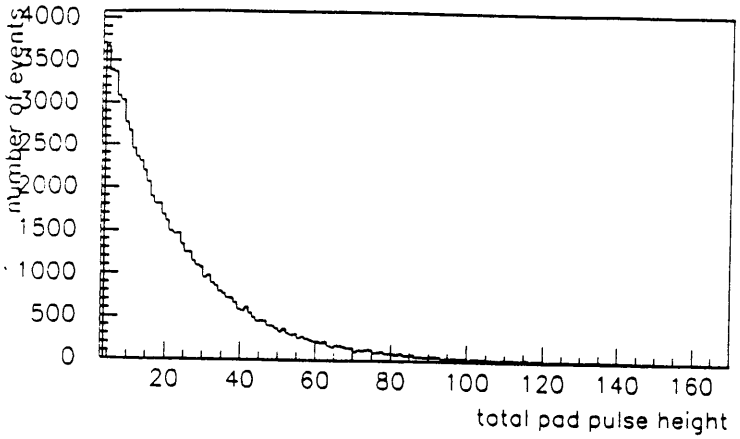

Figure 5: Pulseheight spectra of single electrons.

one. This provides the weighting factors for every pad. For every electron the total charge is generated from a distribution describing the avalanche process. In case of a single electron and low gain it is an exponential of average A_0.

$$P(A) = 1/A_0 * e^{-A/A_0} \tag{5}$$

A_0=20 was used and a threshold A=4 was applied [4], see Fig. 5. The pulseheight pad pattern of an electron is then obtained by multiplying the total charge with the weighting pattern. To get the full event pad pattern all electron pad patterns are summed up.

The various wavelength dependent transmissions and efficiencies of the ingoing components were based on measurements, mostly done by the CERN RD26 project [4].

The window simulated was either made of CaF_2 or quartz. A comparison was also made between different positions of the detector, in front of H3 or after H2 (see Fig. 2). Placing the detector more upstream makes it possible to make it smaller, since the particles are less spread out. In the upstream position the particle tracks are closer, which means that the overlap of photon blobs is increased and separation becomes harder. This can be reduced by making the detector shorter, then the photon blobsize is reduced but also the number of emitted photons.

The following configurations were investigated:

- Position in front of H3 with 100cm radiator length and:
  - CaF_2 window or
  - quartz window
- Position after H2 with with 80cm radiator length and:
  - CaF_2 window or
  - quartz window

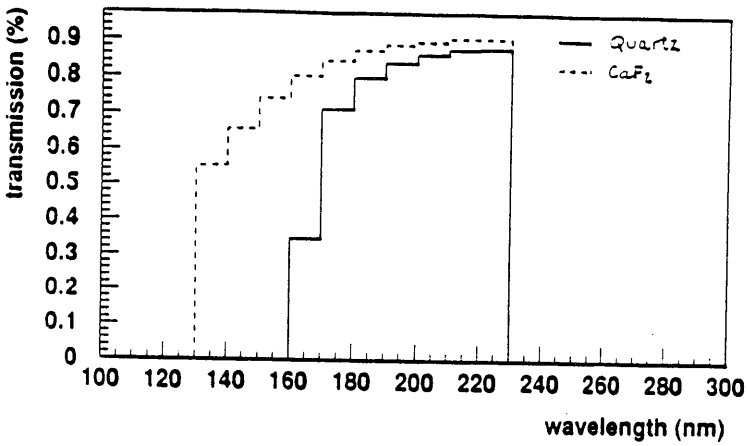

Figure 6: The transmission of quartz and CaF_2 as a function of wavelength.

3.2 Results

The factors of merit achieved for the two different windows were 60 cm^{-1} with CaF_2 and 40cm^{-1} with quartz. This corresponds to 30% less photons detected with the quartz window, which is because it's transmission cuts off earlier when going to shorter wavelengths (See Fig. 6), but the CaF_2 window is considerably more expensive.

One photon gives induction on two or three pads. When the induction is in the corner of a pad (in the look up table, which corresponds to 0.5mm from the next pad) there's still 86% of the induction on the central pad. In Figures 7- 9 a typical event is followed through the different parts of the detector.

A comparison between the photon blobs for the two different positions can be found in Fig. 10. For the H3 position the photon blob is ≈5.5cm and the average number of photons is 11 (the peak for 0 photons are kaon tracks), these values goes down to a blob radius of ≈4.5cm and 9 photons per pion for the H2 position (because of the shorter radiator length).

To analyse the padarray output the number of pads hit and the total integrated pulseheight within a searchradius were calculated. In Fig. 11 this is plotted for pions and kaons respectively. Kaons with a lot of pads hit and a large total pulseheight within the searchradius corresponds to tracks close to a piontrack. In that case the following analysis algorithm is too simple and a more elaborate algorithm should be used.

Identification of the particles was done by simply demanding more than a certain number of pads hit and more than a certain total pulseheight within the searchradius around the particle for it to be identified as a pion. If not it was identified as a kaon. This identification was then compared with the particle's generated (true) type and the detecting capability could be evaluated. To evaluate the results the following definitions were used:

- a = number of generated tracks of a certain type
- b = number of found tracks of the same type
- c = number of found tracks that were correct
- Efficiency: b/a
- Purity: c/b

The results for the different settings are shown in Table 1.

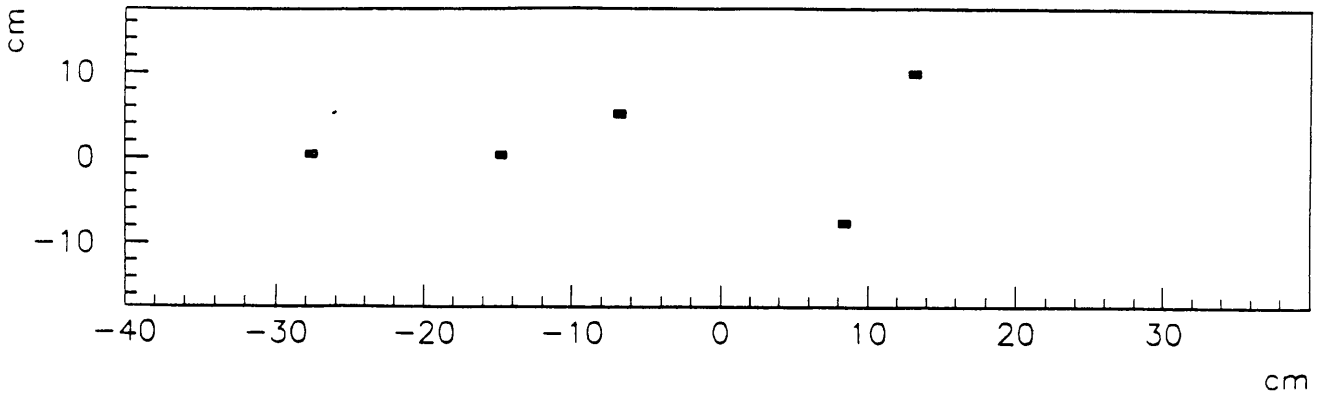

Figure 7: Positions of the particles while exiting the chamber.

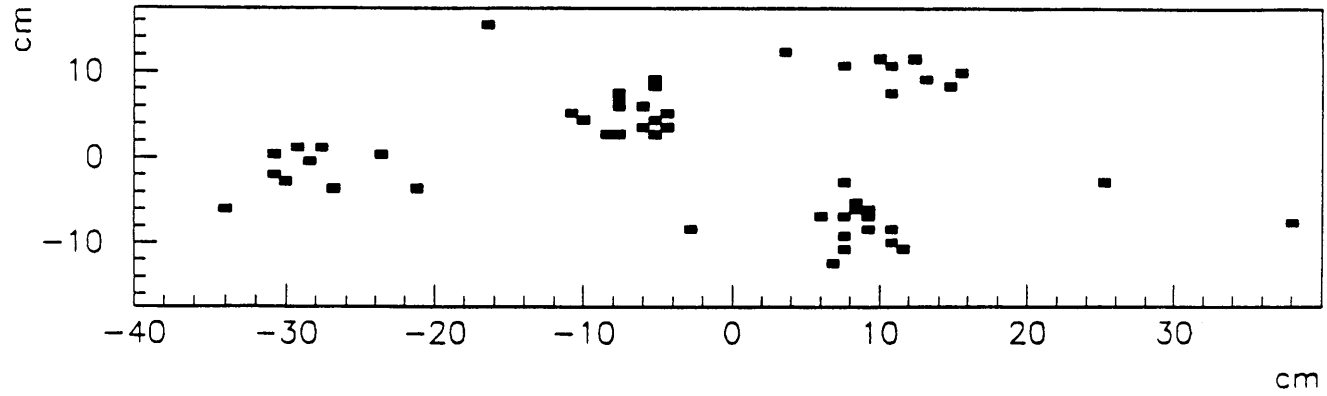

Figure 8: Positions of the photons on the window.

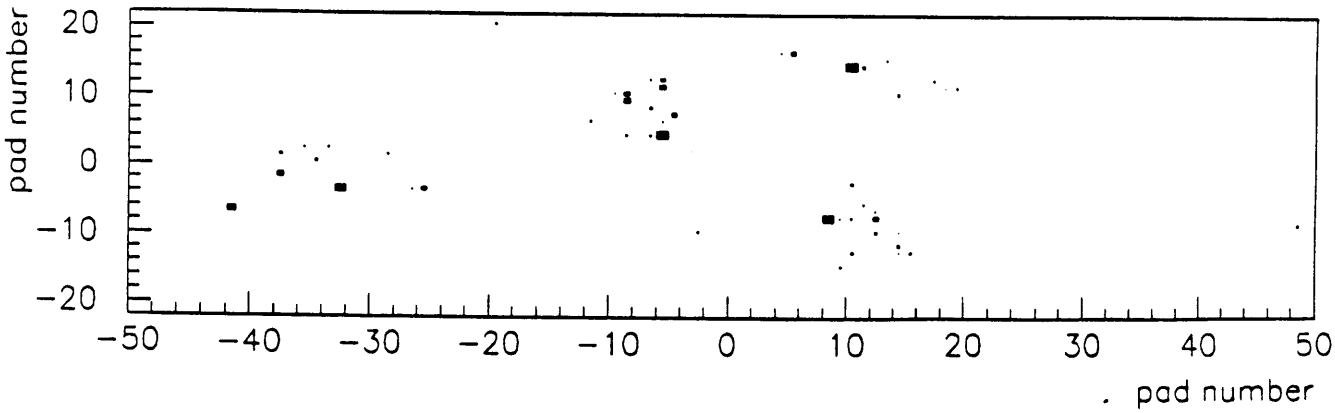

Figure 9: The pad chamber response.

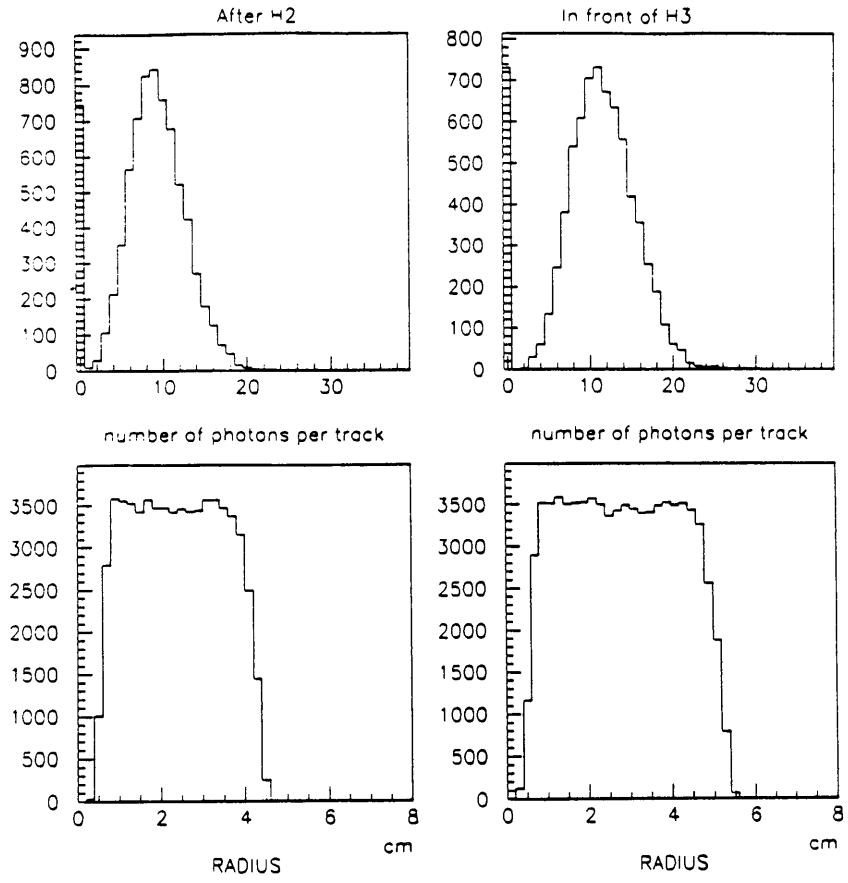

Figure 10: Comparison between the two different positions.

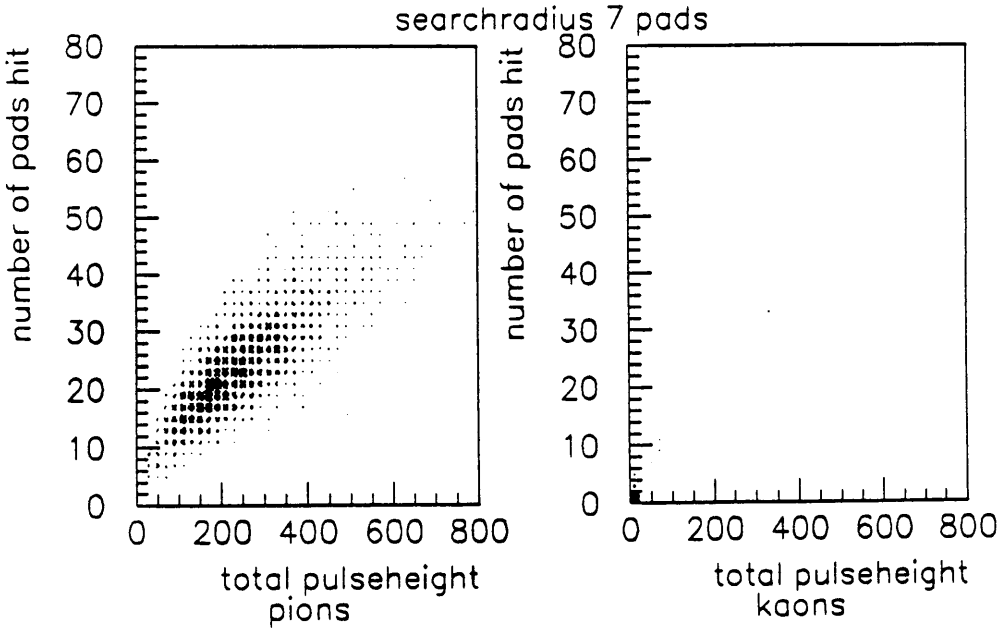

Figure 11: Total number of pads hit versus the integrated pulseheight in a circular area around a particle track measured by the photon chamber.

Table 1: Efficiencies and purities for different settings.

	After H2		In front of H3	
	Quartz	CaF_2	Quartz	CaF_2
pion efficiency	99.0%	99.9%	98.2%	99.9%
pion purity	97.2%	97.3%	98.1%	98.0%
kaon efficiency	76.2%	72.2%	81.4%	85.0%
kaon purity	82.9%	90.9%	87.0%	90.0%
kaon pair event efficiency	43.6%	55.1%	58.5%	71.0%
kaon pair event purity	86.4%	94.4%	91.9%	96.0%

4 Conclusions

Before drawing any conclusions I would like to stress the fact that, for the parameters in Table 1, a gain in purity costs a lot in efficiency and that this should be kept in mind when comparing the different settings.

A significantly better kaon identification is achieved in the position in front of H3 than after H2. The results are worse for a quartz window than for a CaF_2 window, because of the 30% decrease in the number of photons. It should also be noted that the results with a chamber equipped with CaF_2 windows positioned after H2 is comparable with the one's of a chamber with quartz windows positioned in front of H3.

5 Acknowledgements

I am grateful to my supervisor A. Franz for his help and patience and to S. Esumi and J. Sorensen with whom parts of this work was carried out. Many thanks to F. Piuz for valuable discussions on the properties of pad chambers. I also would like to thank C. Fabjan and other NA44 collaborators for their support during this study.

References

[1] J.D. Jackson *Classical Electrodynamics*, 2nd ed. John Wiley & sons (1972).

[2] Na44 Collaboration *Proposal for a focussing spectrometer for one and two particles*, CERN preprint CERN/SPSC/88-37 SPSC/P239 (1988).

[3] F. Sauli *Principles of operation of multiwire proportional and drift chambers*, CERN preprint CERN 77-09 (1977).

[4] F. Piuz *NA44,RD26*, private communication.